

# PHYSICAL REVIEW C

## NUCLEAR PHYSICS

THIRD SERIES, VOLUME 32, NUMBER 5

NOVEMBER 1985

### $^{17}\text{O}(\vec{p},t)^{15}\text{O}$ reaction at 90 MeV

K. F. von Reden, W. W. Daehnick, S. A. Dytman, and R. D. Rosa

*Department of Physics and Astronomy, University of Pittsburgh, Pittsburgh, Pennsylvania 15260*

J. D. Brown,\* C. C. Foster, and W. W. Jacobs

*Indiana University Cyclotron Facility, Bloomington, Indiana 47405*

J. R. Comfort

*Department of Physics, Arizona State University, Tempe, Arizona 85287*

(Received 13 May 1985)

Differential cross sections and analyzing powers of the  $^{17}\text{O}(\vec{p},t)$  reaction were measured over the angular range from  $5^\circ$  to  $55^\circ$  at  $T_p = 89.7$  MeV. The data for transitions to five residual states of  $^{15}\text{O}$  are compared with calculations in the finite-range and zero-range distorted-wave Born approximation. The distorting potential parameters were obtained from optical-model analyses of elastic proton and helion scattering. The  $(\vec{p},t)$  cross sections are underpredicted by the finite-range calculations and overpredicted by zero-range calculations based on standard normalizations. The reproduction of the analyzing powers is only fair. Two-step calculations of the type  $(\vec{p},d;d,t)$  were performed in a zero-range, second-order distorted-wave Born approximation. The ground state and six one-particle, one-hole states of  $^{16}\text{O}$  were taken into account as intermediate states. Consistent improvement in the prediction of the data was not obtained.

### I. INTRODUCTION

Two-nucleon-transfer reactions have been extensively investigated and used for the study of nuclear structure at various projectile energies. Much of the interest in them lies in their sensitivity, in principle, to the relative phases of the microscopic configurations of the observed states. This sensitivity is often enhanced by measurements of analyzing powers. However, it has often been difficult to make detailed interpretations of the experimental data because of considerable uncertainties in the description of the reaction mechanisms.

Previous  $(\vec{p},t)$  and  $(\vec{p},^3\text{He})$  experiments on  $p$ -shell and light  $sd$ -shell nuclei at low incident energies showed that the distorted-wave Born approximation (DWBA) can often correctly predict cross sections at forward angles, whereas the predictive quality for analyzing powers was limited.<sup>1,2</sup> A good reproduction of the data has usually been achieved only for transitions of a collective nature. Conventional DWBA predictions of the cross sections are found to depend primarily on the transferred angular momentum. The observed analyzing powers, however, can be significantly different for transitions which have the same  $L$  and  $J$  transfer, but a different microscopic structure.<sup>1</sup> A similar observation has been made in analyses of

$^{48}\text{Ca}(\vec{t},p)$  and  $^{207}\text{Pb}(\vec{t},p)$  data.<sup>3</sup>

The correct treatment of the reaction mechanism in the DWBA is still problematic. Among the issues that have been raised are the choices of parameter families of optical-model parameters, the validity of the zero-range approximation, and the composite-particle wave functions used in finite-range treatments. The importance of two-step processes in two-nucleon transfer reactions has also been noted in various previous investigations.<sup>4-11</sup> These, in addition, have raised questions of the relative normalization and phase relations between one- and two-step paths as well as nonorthogonality corrections.<sup>12,13</sup>

Within the framework of the DWBA, the full microscopic interpretation of the two-nucleon-transfer process requires knowledge of the initial-, intermediate-, and final-state wave functions as well as specification of the various interactions. In order to focus most directly on the role of the reaction mechanisms, target nuclei need to be restricted to those that have only a few particles or holes outside closed shells, so that the wave functions are calculable.

The present paper reports on a study of the  $^{17}\text{O}(\vec{p},t)^{15}\text{O}$  reaction at 89.7 MeV. In this case, the target nucleus and residual nucleus represent well-understood one-particle and one-hole configurations near the closed-shell  $^{16}\text{O}$  core.

An earlier study of the (p,t) and (p,<sup>3</sup>He) reactions on <sup>17</sup>O by Olson and Brown<sup>14</sup> with unpolarized protons of 40 MeV focused on relative cross sections of one-hole isobaric analog states of <sup>15</sup>O and <sup>15</sup>N. The data were interpreted in terms of one-step, zero-range DWBA calculations. The present data will be compared with absolute cross sections computed in the one-step, finite-range (FR) DWBA. We also investigate the issue of two-step transfer mechanisms by use of the second-order DWBA in zero range (ZR).

## II. EXPERIMENTAL PROCEDURES

Measurements of the cross-section and analyzing-power angular distributions were performed at the Indiana University Cyclotron Facility (IUCF) by using a polarized proton beam of 89.7 MeV. The average beam polarization was typically about 75% at a beam current of about 100 nA. The polarization was checked periodically by performing asymmetry measurements of elastic proton scattering from <sup>4</sup>He. The polarimeter gas cell was located between the injector and main cyclotrons and the beam energy at that point was 7.84 MeV. Earlier elastic-scattering analyses at IUCF have shown that the polarization loss in the last stage of acceleration is less than 0.02.<sup>15</sup> More recent investigation under conditions of single-turn extraction indicate that the depolarization at times can be as much as twice this amount for protons.<sup>16</sup> The spin polarity was flipped in 30-sec cycles to avoid systematic errors from slowly varying instabilities. At forward scattering angles, a split Faraday cup located inside the scattering chamber allowed both the beam current and the horizontal positional stability of the beam to be monitored. At angles larger than 25°, an external Faraday cup was located 7 m downstream from the target position.

The target was a silicon dioxide slurry with thickness 0.84 mg/cm<sup>2</sup> and an oxygen isotopic ratio 16/17/18 of 0.20/0.55/0.25. From elastic proton scattering measurements, the relative uncertainty in the isotope ratio was estimated to be about ±5% and the absolute error in the target thickness to be about 15%. For the major part of the measurements, the target stability was monitored with a plastic-scintillator telescope located at a laboratory angle of 12° and a distance of 1.4 m from the target.

The reaction products were analyzed with a quadrupole-dipole-dipole-multipole (QDDM) magnetic spectrometer. A helical delay line (helix) counter served as a positron-sensitive focal plane detector. Two thin plastic-scintillator detectors were placed behind the helix detector for use in particle identification. The 60-cm-wide helix detector covered an excitation energy range of about 5 MeV. Hence two magnetic field settings had to be taken at each angle to cover the 10-MeV excitation range of interest. The data were taken over the angular range from 5° to 55° in steps of 5°. The spectrometer angular resolution was 1.36°. This value was used in the calculations of differential cross sections and analyzing powers to account for the small errors due to the summation over a finite angular range.

Figure 1 shows an example of the triton spectra measured at a laboratory angle of 10°. An overall energy reso-

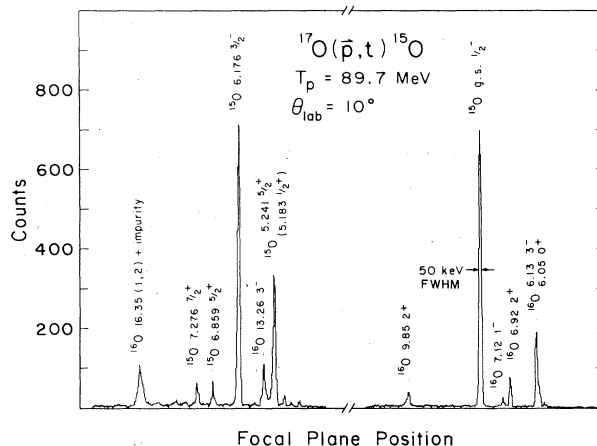


FIG. 1. A <sup>17</sup>O( $\bar{p}$ ,t)<sup>15</sup>O spectrum obtained at a laboratory angle of 10°. The figure is a composite of two adjacent momentum bites of the QDDM magnetic spectrometer.

lution of about 50 keV was obtained with a beam energy spread of 35 keV. As a result of the (p,t)  $Q$  values for the difference target isotopes, only triton groups from the <sup>17</sup>O(p,t) and <sup>18</sup>O(p,t) reactions can be found in the spectrum. The typical 10% dead time of the data-acquisition system was measured by feeding a pulser signal triggered by the current integrator through the entire electronics and computer system and comparing the accumulated counts of the pulser peak in the computer-generated spectrum with the directly scaled number of pulser signals. The absolute error of the cross sections obtained was estimated to be about 15%, primarily due to the uncertainty in target thickness. The error bars displayed with the data in the following sections contain all random errors but are dominated by the counting statistics.

## III. DWBA ANALYSIS

Two-nucleon-transfer in the framework of the DWBA has been discussed elsewhere in detail.<sup>17,18</sup> Some of the known problems with the application of DWBA to two-nucleon-transfer reactions have already been mentioned in the Introduction. Additional difficulties may arise from an increase in momentum mismatch due to the relatively high bombarding energy used in this study. There have been few studies of (p,t) reactions above 50 MeV, and even fewer with polarized beams. There are reports of "spectacular" failures in DWBA analyses for <sup>24</sup>Mg(p,d) and <sup>60</sup>Ni(p,d) at  $E_p=94$  MeV.<sup>19,20</sup> Significant discrepancies with the normalization of (p,t) reactions on <sup>12</sup>C, <sup>54</sup>Fe, and <sup>208</sup>Pb at 80 MeV, in comparison with lower-energy data, have also been noted.<sup>21</sup>

### A. Optical-model potentials

The optical potential parameters for the entrance and exit channels were determined by optical-model (OM) fits to elastic-scattering data. The <sup>17</sup>O( $\bar{p}$ ,p<sub>0</sub>) elastic-scattering angular distributions at 89.7 MeV were measured directly in the present experiment. Figure 2 displays the OM fit

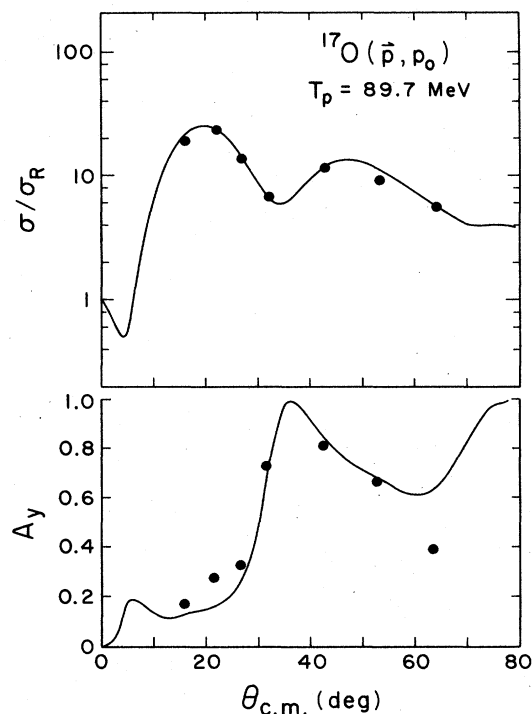


FIG. 2. Differential cross sections and analyzing powers for elastic proton scattering from  $^{17}\text{O}$  as measured in the present work. The solid curves are results of an OM fit with search code CUPID (Ref. 22). The parameter values are listed in Table I.

to the cross sections and analyzing powers as obtained with the OM search code CUPID.<sup>22</sup>

Since no triton elastic-scattering data are available at bombarding energies above 20 MeV, recent measurements<sup>23</sup> of  $^3\text{He}$  elastic scattering from  $^{16}\text{O}$  at 78.6 MeV were used to determine the exit channel optical potential. Figure 3 shows the fits to the data obtained for two parameter sets that differ principally in the depth of the real part of the central potential. A shallow ( $S$ ) and a deep ( $D$ ) potential gave an almost equivalent fit over the given angular range. It has previously been found, however, that while the shallow potential gives a better fit to the elastic-scattering data at large angles, it produces very poor descriptions of transfer reactions when used in the DWBA. The optical-model parameter sets used in the present DWBA calculations are displayed in Table I. The convention for the parametrization is described in Ref. 24. It should be noted that the values listed for the spin-orbit potentials assume that the factor  $(\hbar/m_\pi c)^2 = 2.0 \text{ fm}^2$  is provided by the code and that the operator is  $(\vec{1} \cdot \vec{s})$ . Corrections for an isovector potential in the triton- $^{15}\text{O}$  channel were found to be small and were neglected.

Previous studies of two-nucleon-transfer reactions have indicated that DWBA predictions can be quite sensitive to the choice of the composite projectile OM potential parameters.<sup>25</sup> As an illustration of the variety of possible parameter sets, the volume integrals per nucleon for the real part of the central potential are plotted in Fig. 4

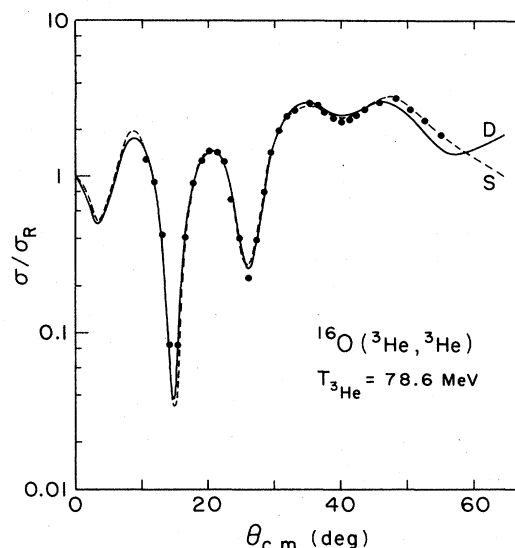


FIG. 3. Differential cross sections for  $^3\text{He}$  elastic scattering from  $^{16}\text{O}$  at 78.6 MeV from Ref. 23. The curves are results of OM fits for two differential potential sets. The parameter values for the deep potential  $D$  (solid curve) and for the shallow potential  $S$  (dashed curve) are listed in Table I.

against projectile energy. Folding-model calculations based on proton and deuteron optical potentials indicate that this integral should be a smooth and almost linear function of the projectile energy. An extrapolation of the Becchetti-Greenlees global parameters<sup>26</sup> to higher projectile energies and lower target mass, as indicated by the dashed straight lines in Fig. 4 for tritons and helions, agrees more generally with the "deeper" potentials. A similar comparison cannot easily be made for the imaginary part of the potential because of the variety of different geometrical parametrizations that are used in the literature.

The sensitivity of the calculated absolute one-step (p,t) cross sections and analyzing powers to the variation of the

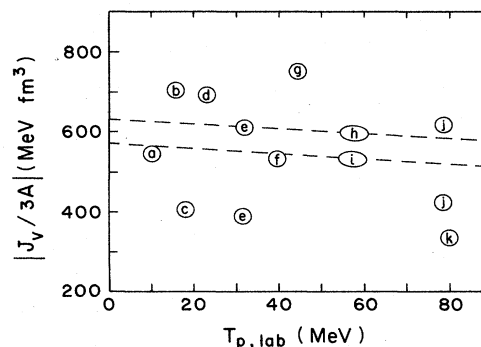


FIG. 4. Volume integrals per nucleon for the real central part of optical-model potentials for mass-three projectiles on oxygen targets versus the projectile energy derived from various previous investigations: (a) Ref. 27; (b) Ref. 28; (c) Ref. 29; (d) Ref. 2; (e) Ref. 30; (f) Ref. 14; (g) Ref. 1; (h) Ref. 26 for tritons, extrapolated; (i) Ref. 26 for helions, extrapolated; (j) OM fits to data from Ref. 23; (k) Ref. 31 (for carbon target).

TABLE I. Values of optical model potential parameters used in the DWBA calculations.

	$V$	$r$	$a$	$W$	$W_D$	$r_i$	$a_i$	$V_{so}$	$r_{so}$	$a_{so}$	$\chi^2$
$p^a$	33.0	1.20	0.64	10.3		1.34	0.66	6.18	1.08	0.49	4.7
$d^b$	67.1	1.17	0.87	8.46	6.16	1.33	0.71	9.27	1.07	0.66	
$t(BG)^c$	150.0	1.20	0.72	23.6		1.40	0.84	10.0	1.20	0.72	
$\tau, t(S)^d$	99.2	1.24	0.77	1.24	15.8	1.40	0.71	3.30	0.91	0.49	1.9
$\tau, t(D)^d$	205.0	1.08	0.72		14.9	1.35	0.67	5.67	0.73	0.67	3.3

<sup>a</sup>Result of OM fit (Fig. 2) to data from  $^{17}\text{O}(\vec{p}, p_0)$  at 87.9 MeV.

<sup>b</sup>Taken from Ref. 24.

<sup>c</sup>Parameters from Ref. 26 extrapolated with respect to target mass and bombarding energy.

<sup>d</sup>Result of OM fit (Fig. 3) to data (Ref. 23) from  $^{16}\text{O}(^3\text{He}, ^3\text{He}_0)$  at 78.6 MeV.

exit channel potential parameters was investigated with several finite-range DWBA calculations. Figure 5 shows the ground-state transition data together with calculated curves for the various potential sets. The experimental cross section at  $\theta_{c.m.} = 23^\circ$  was chosen as a reference point

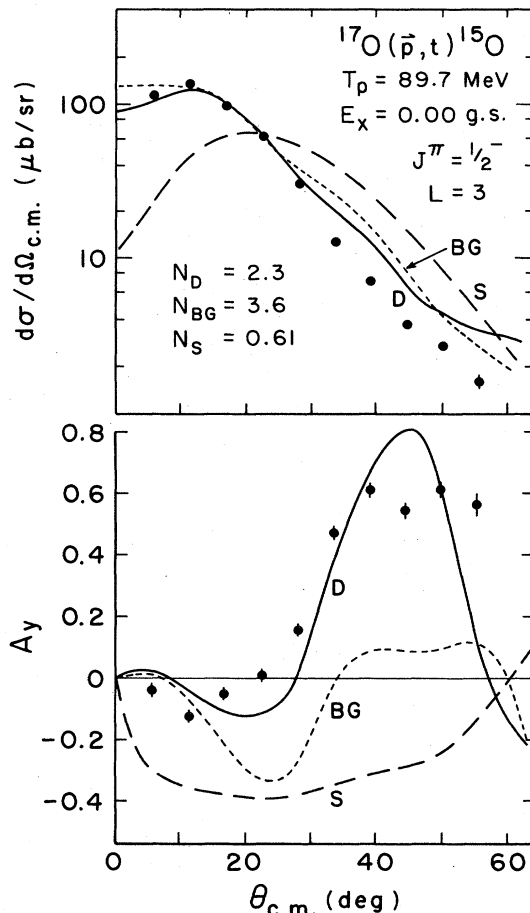


FIG. 5. Sensitivity of finite-range, one-step, two-nucleon-transfer DWBA calculations to the choice of the exit channel scattering potential. The figure shows differential cross sections and analyzing powers of the  $^{17}\text{O}(\vec{p}, t)^{15}\text{O}$  ground-state ( $J^\pi = \frac{1}{2}^-$ ) transition compared with DWBA curves calculated for three different exit channel optical potentials as described in the text. The cross-section curves were normalized to the data at  $\theta_{c.m.} = 23^\circ$  by the factors given in the figure.

for the normalization of the several calculated curves. The calculations based on the shallow potential  $S$  overpredict the cross sections and do not reproduce the shapes of either the cross-section or analyzing-power angular distributions. The calculations with the deep potential  $D$  underpredict the cross sections but reproduce the shape of the angular distributions fairly well. For comparison, calculations resulting from the use of the extrapolated Becchetti-Greenlees (BG) parameters are also shown in Fig. 5.

Although the choice of appropriate OM potential sets remains uncertain, the calculations presented in the following sections were made with potential  $D$  in the exit channel. Test calculations with potential  $S$  gave clearly inferior results within the constraints of the configuration space used in this work.

## B. Reaction calculations

Calculations of the  $^{17}\text{O}(\vec{p}, t)$  reaction were made with the codes FRUCK2 (Ref. 32) and CHUCK3 (Ref. 33). The finite-range DWBA and FRUCK2 makes use of the description of the triton by Tang and Herndon,<sup>34</sup> which has been successfully applied to  $(p, t)$  and  $(p, ^3\text{He})$  reactions at lower projectile energies. The light-ion form factor incorporates a hard-core term and includes all proper spin normalizations.<sup>35</sup> The code CHUCK3 was used for both the zero-range, one-step and two-step DWBA calculations. It uses the Bayman-Kallio prescription<sup>36</sup> to produce a radial form factor for the microscopic two-nucleon transfer. For the two-step calculations, it was found sufficient to use the code in the mode of second-order DWBA. The bound-state wave functions of the transferred nucleons were generated in both codes with a Woods-Saxon potential well ( $r = 1.25$  fm,  $a = 0.65$  fm), which was adjusted in depth to give half the two-nucleon separation energy.

The two-step calculations were performed in order to estimate the contributions from the dominant sequential-transfer process of the form  $(p; d; d, t)$ . There has been considerable discussion<sup>5,12,13</sup> about the correct summation of amplitudes for the one-step and the various two-step channels arising from the fact that the CHUCK3 program does not automatically supply all needed phases. Within a given model of nuclear structure and reaction mechanism, of course, there is no freedom of choice for the relative phases. They must, in addition, be matched to the inter-

TABLE II. Spectroscopic amplitudes  $C\mathcal{S}^{1/2}$  for the  $^{17}\text{O}$  one-particle to  $^{15}\text{O}$  one-hole transitions.

$^{15}\text{O}$ final state	One-step transfer		Two-step transfer via $^{16}\text{O}$ g.s. $0^+$	Two-step transfer via $^{16}\text{O}$			
	$L=1$	$L=3$		$1^-$	$2^-$	$3^-$	$4^-$
g.s., $J^\pi = \frac{1}{2}^-$		$-\sqrt{7/6}$	$\sqrt{2}$		$-\sqrt{5/6}$	$-\sqrt{7/6}$	
6.176, $J^\pi = \frac{3}{2}^-$	$-\sqrt{1/2}$	$-\sqrt{7/6}$	2	$-\sqrt{1/2}$	$-\sqrt{5/6}$	$-\sqrt{7/6}$	$-\sqrt{3/2}$

nal conventions of the code being used. In the present case, the phases were carefully evaluated along the lines described in Ref. 5. The spectroscopic amplitudes are listed in Table II. Standard zero-range normalizations  $D_0$  were used. The values for use with the code CHUCK3 are the following:  $D_0(p,d) = 122.5 \text{ MeV fm}^{3/2}$ ,  $D_0(d,t) = -225 \text{ MeV fm}^{3/2}$ , and  $D_0(p,t) = -1560 \text{ MeV fm}^{3/2}$ .

### C. Shell-model structure

In the present study, the  $^{17}\text{O}$  ground state ( $J^\pi = \frac{5}{2}^+$ ) was assumed to be an almost pure single-particle state with one neutron in the  $d_{5/2}$  shell outside the closed  $^{16}\text{O}$  core. This assumption is supported by three observations: (i) the electric quadrupole moment of  $^{17}\text{O}$  is close to zero; (ii) the magnetic moment agrees with the Schmidt lines; and (iii) neutron scattering from  $^{16}\text{O}$  yields a spectroscopic strength of 91% of the single-particle value.<sup>37</sup> The  $^{17}\text{O}(\bar{p},t)$  reaction predominantly populates the neutron  $p$ -shell hole states in  $^{15}\text{O}$ , the  $J^\pi = \frac{1}{2}^-$  ground state and the  $J^\pi = \frac{3}{2}^-$  excited state at  $E_x = 6.176 \text{ MeV}$ . The  $^{15}\text{O}$  excited states at 5.241 MeV ( $\frac{5}{2}^+$ ), 6.859 MeV ( $\frac{5}{2}^+$ ), and 7.276 MeV ( $\frac{7}{2}^+$ ) are assumed to be neutron  $d_{5/2}$  particle,  $p$ -shell two-hole states. The  $\frac{1}{2}^+$  state reported<sup>38</sup> at 5.183 MeV was not observed in the present experiment.

## IV. RESULTS

### A. One-step analysis

Zero-range and finite-range one-step-transfer calculations for the five  $^{15}\text{O}$  states of the present study are shown together with the data in Figs. 6 and 7. Only the  $\frac{1}{2}^-$  ground state and the  $\frac{7}{2}^+$  state ( $E_x = 7.276 \text{ MeV}$ ) have unique  $L$ -transfer values, which are 3 and 2, respectively. The  $\frac{3}{2}^-$  and the  $\frac{5}{2}^+$  states can be reached with mixtures of  $L=1$  and 3, and  $L=0$  and 2, respectively. The shapes of the angular distributions for the one-hole states are approximately reproduced by both sets of calculations. However, the absolute values of the FR predictions are smaller than the data by about a factor of 2, whereas the ZR results are too large by a factor of about 3.5.

The underprediction of the cross sections by the FR calculations may be expected if other contributions to the reaction mechanism are of similar magnitude as the one-step part and interfere constructively. On the other hand, the overprediction by the ZR calculations may be a consequence of inappropriate values of  $D_0$  which have been computed for relatively low momentum transfers. The momentum-transfer dependence of an effective ZR normalization has been discussed in a recent study of the

( $p,d$ ) reaction on  $p$ - and  $sd$ -shell nuclei at 800 MeV.<sup>39</sup> Based on a realistic deuteron wave function,  $D_0$  has been shown to decrease by as much as a factor of 2 for an increase of the momentum transfer to  $2 \text{ fm}^{-1}$ . Since the

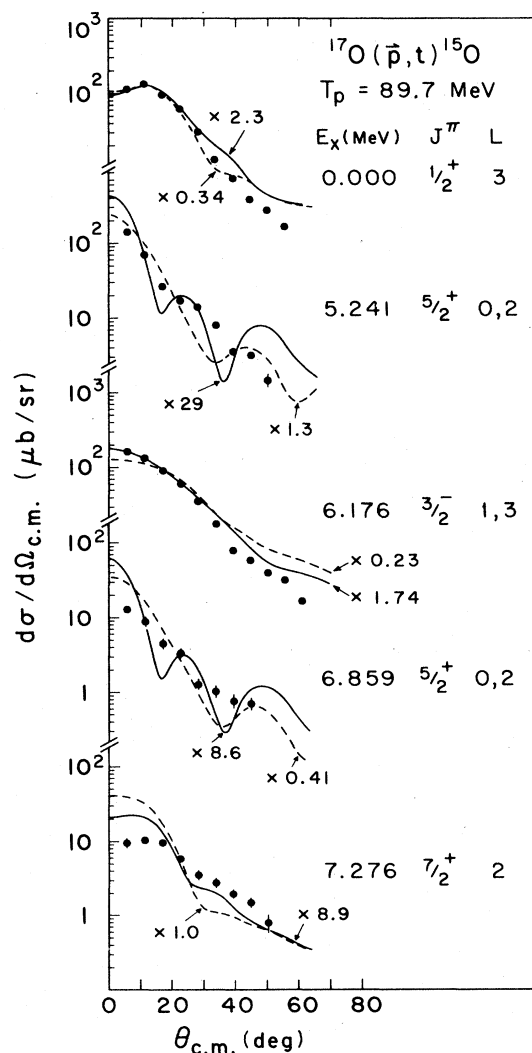


FIG. 6.  $^{17}\text{O}(\bar{p},t)^{15}\text{O}$  differential cross sections for the five residual nuclear states of  $^{15}\text{O}$ . The FR and ZR one-step transfer predictions are displayed as the solid and dashed curves, respectively. For the one-particle to one-hole transitions, the spectroscopic amplitudes from Table II were used. For the other transitions, spectroscopic amplitudes  $C\mathcal{S}^{1/2}$  from Ref. 40 were used, assuming one-particle, two-hole and final-state configurations. The curves were renormalized by the factors given in the figure.

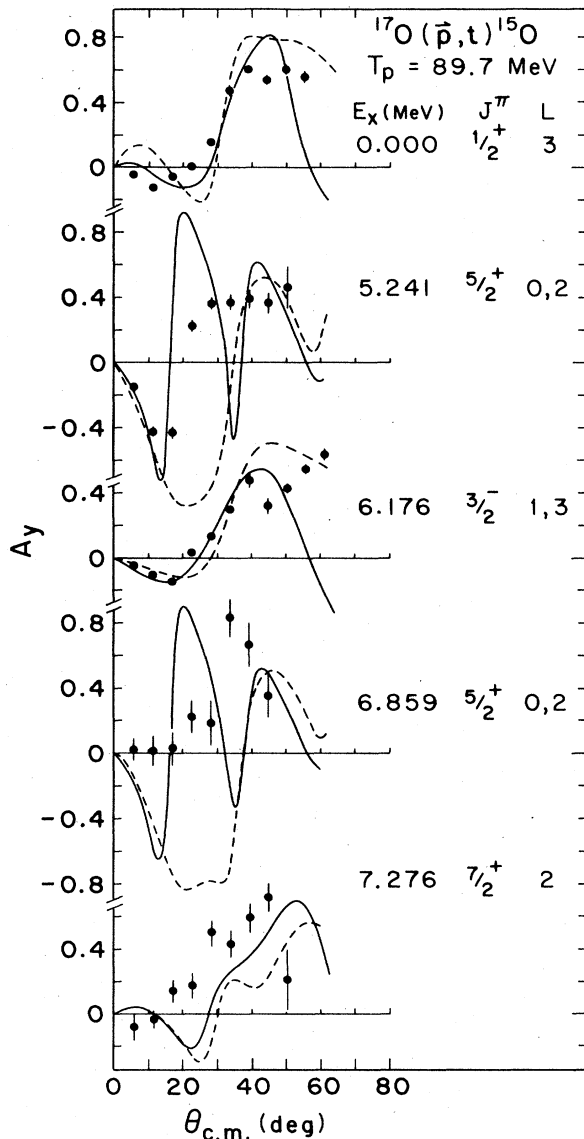


FIG. 7.  $^{17}\text{O}(\bar{p}, t)$  analyzing-power angular distributions for the five states as displayed in Fig. 6. The curves result from the same calculations as described in the caption to Fig. 6.

momentum transfers encountered in the present study for the light-ion systems are of the order of  $1 \text{ fm}^{-1}$ , a considerable decrease of  $D_0$  can be expected from the use of a realistic triton wave function.

The large sensitivity of  $D_0$  to the detailed structure of the composite particle wave functions underlines the importance of a full finite-range treatment at increasing momentum transfers. The validity of zero-range calculations appears to be questionable and the results of such calculations have to be interpreted with caution.

The steep forward-angle peaking of the cross sections and the large negative analyzing powers at forward angles imply a predominant  $L=0$  signature for the  $5/2^+$  state at 5.241 MeV. By using  $L=0$  and  $L=2$  spectroscopic factors  $\mathcal{S}_0$  and  $\mathcal{S}_2$  from shell-model calculations<sup>40</sup> based on

a full  $p$ - and  $sd$ -shell configuration space for the contributions to the 5.241-MeV state, the FR DWBA calculations are found to have too much structure compared to the data. This result indicates that the ratio of  $\mathcal{S}_0$  to  $\mathcal{S}_2$  is too high. On the other hand, the experimental analyzing powers for this state display the large negative values at forward angles predicted by both codes for a pure  $L=0$  transition density. The ZR predictions, which do not have as much oscillatory structure in the cross sections as the FR results, produce analyzing powers that deviate substantially from both the FR prediction and the data between  $15^\circ$  and  $30^\circ$ .

The analyzing powers for the weaker second  $5/2^+$  state at 6.859 MeV do not show large negative values at forward angles. Although the  $\mathcal{S}_0/\mathcal{S}_2$  ratio from Ref. 40 is smaller for this state than for the state at 5.241 MeV, the FR predictions of the shapes of both the cross-section or analyzing-power angular distributions are poor. Furthermore, the ZR calculations for the analyzing powers again disagree with the FR results and the data over the angular range of  $15^\circ$ – $30^\circ$ . In order to estimate the  $L=2$  admixtures, pure  $L=2$  FR predictions are plotted for the two  $5/2^+$  states in Fig. 8. Clearly, larger  $L=2$  admixtures than given by the shell model calculations would give a better overall representation of the data.

The cross-section data for the  $7/2^+$  state at 7.276 MeV exhibit a rather flat angular distribution. Both of the ZR and FR calculations predict a steeper forward-angle peaking than shown by the data. The predictions of the analyzing powers by both codes are of similar quality and represent only the gross features of the data.

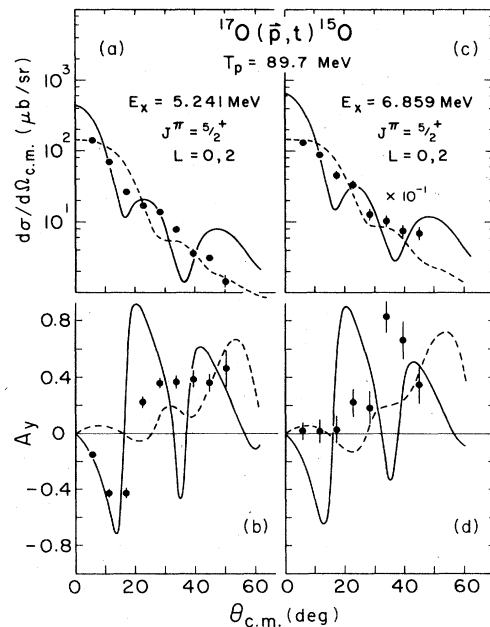


FIG. 8. One-step, finite-range predictions for the two  $J^\pi = 5/2^+$  states of  $^{15}\text{O}$  with spectroscopic amplitudes taken from full  $p$ - and  $sd$ -shell model calculations (Ref. 40). The solid lines are the full results, the dashed curves show the pure  $L=2$  results.

### B. Two-step calculations

The effect of the inclusion of sequential ( $\bar{p},d;d,t$ ) pick-up processes in ZR second-order DWBA calculations was investigated for the transfers from the simple one-particle states of  $^{17}\text{O}$  to the one-hole states of  $^{15}\text{O}$  through intermediate (1p-1h) states in  $^{16}\text{O}$ . Since the exact structures of the positive-parity states in  $^{15}\text{O}$  are uncertain, two-step contributions were not explicitly considered for them. The removal of the  $d_{5/2}$  neutron from  $^{17}\text{O}$  leads to the  $0^+$  ground state of  $^{16}\text{O}$ . Final  $^{15}\text{O}$  states with  $J^\pi = \frac{1}{2}^-$  and  $\frac{3}{2}^-$  are reached by a second pickup of a  $p_{1/2}$  or  $p_{3/2}$  neutron, respectively. Reversing the order, the pickup of a  $p$ -shell neutron first leads to intermediate  $^{16}\text{O}$  1p-1h states of the multiplets  $|d_{5/2},(p_{1/2})^{-1}\rangle_{2,3,-}$  and  $|d_{5/2},(p_{3/2})^{-1}\rangle_{1-,2-,3-,4-}$ . The energy centroids of these multiplets were taken from Ref. 41. Results of the ZR two-step calculations, including the above intermediate states, are presented in Figs. 9 and 10 for the ground state and the 6.176-MeV states.

The large overprediction of the one-step transfer cross

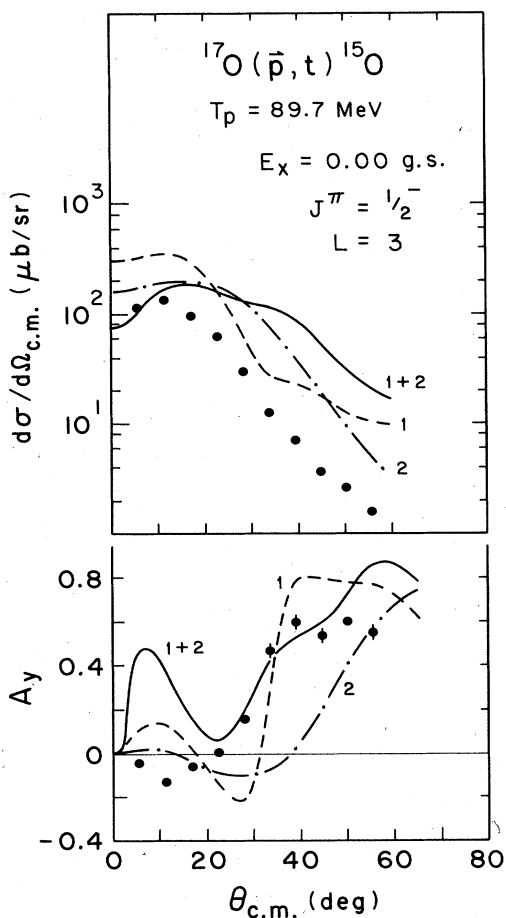


FIG. 9.  $^{17}\text{O}(\bar{p},t)$  angular distributions for the transfer to the ground state,  $J^\pi = \frac{1}{2}^-$ , of  $^{15}\text{O}$  in comparison with curves from zero-range, one-step (dashed) and two-step (dashed-dotted) calculations. The solid curves are the result of a coherent sum of one-step and two-step amplitudes.

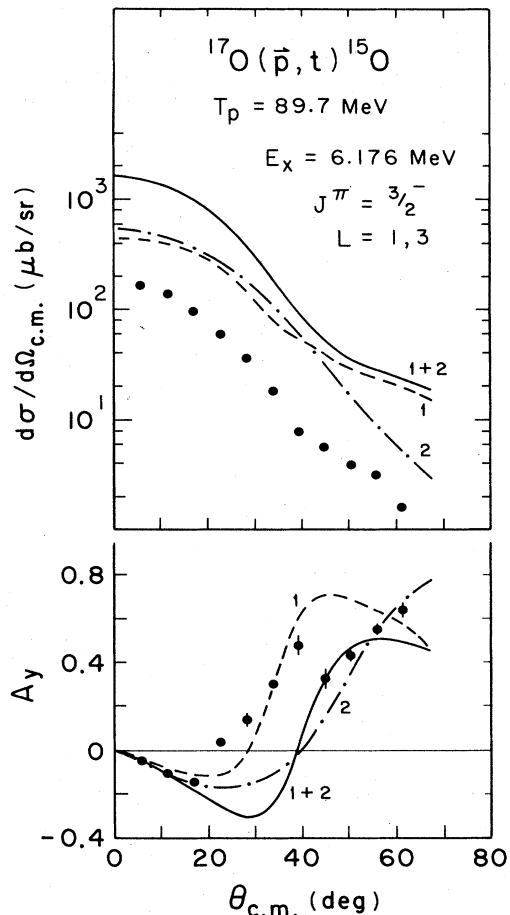


FIG. 10.  $^{17}\text{O}(\bar{p},t)$  angular distributions for the transfer to the 6.176-MeV,  $J^\pi = \frac{3}{2}^-$  state of  $^{15}\text{O}$ . The various curves are the result of calculations as described in the caption to Fig. 9.

sections by ZR calculations raises the question of how they should be normalized for combining with the two-step contribution. As shown in Figs. 9 and 10, the predicted cross sections obtained from the three or five coherently summed two-step transfer amplitudes are of the same magnitude as that obtained from one-step ZR calculations. Hence the two-step contributions to the reaction process cannot be neglected. The FR one-step calculations also suggest that about 50% of the transfer cross section may be due to the two-step mechanism or more complicated processes.

For the ground state transition, pure  $L=3$  ZR one-step calculations can approximately reproduce the shapes of the cross-section and analyzing-power angular distributions. The coherent addition of the two-step contributions, based on the spectroscopic amplitudes of Table II, leads to inferior predictions, as shown in Fig. 9. Strong interference effects drastically change the shapes of the angular distributions. Since the one-step cross sections are overpredicted by the ZR calculations (compared to the FR calculations) they have to be renormalized. A similar renormalization is expected to be necessary for the two-step contributions. However, with the constraint that the

relative spectroscopic amplitudes and phases in the two-step channels remain unchanged, no renormalization of the one-step contribution could be found that would result in better agreement between the calculated curves and the data.

The one-step prediction for the mixed  $L=1$  and 3 transfer to the  $\frac{3}{2}^-$  state at 6.176 MeV was found to be of similar quality as that for the ground-state transition. However, in this case, the coherent summation of the one- and two-step amplitudes yields an overall enhancement of the cross sections. Figure 10 displays the results in which the cross sections are overpredicted by about a factor of 10. Although the shape of the cross-section angular distribution is very well reproduced, the prediction for the analyzing powers is significantly worse than for the one-step result. Again, attempts to renormalize the calculations, leaving the relative spectroscopic amplitudes from Table II for the two-step channels unchanged, led to no improvement in the reproduction of the data.

It should be reiterated that single-nucleon-transfer cross sections are also overpredicted by ZR calculations at increasing momentum transfers.<sup>39</sup> Hence, the precise ZR renormalization for the sequential pick-up channels is not known. An arbitrary change of the relative phases of the one-step and two-step amplitudes can in some cases (but not consistently) improve the agreement between the calculations and data. However, such calculations are at best inconclusive because of the other large uncertainties in the ZR two-step calculations. For example, nonorthogonality effects were not taken into account in the calculations. Other two-step processes such as  $(\vec{p}, p', t)$  or  $(\vec{p}, d', t)$ , where  $d'$  is the deuteron spin singlet state, were explored using constants distributed with CHUCK3. Contributions from the latter processes were found to be at least one order of magnitude smaller than the processes discussed above and were neglected.

## V. DISCUSSION AND SUMMARY

Most experimental and theoretical investigations of the past decade have led to the conclusion that sequential transfer mechanisms play an important role in two-nucleon-transfer reactions. From various analyses<sup>10,11,42</sup> of the unnatural-parity transition  $^{208}\text{Pb}(p,t)^{206}\text{Pb}$  ( $J^\pi=3^+$ , 1.34 MeV), it has become clear that the mere reproduction of cross sections does not suffice to resolve the problem of the  $(p,t)$  reaction mechanism. A correct prediction of analyzing-power data seems to be essential.

The Tsukuba group<sup>6</sup> has focused on the reproduction of analyzing-power angular distributions for the  $(\vec{p}, t)$  reaction on Ni, Zr, Mo, Ru, Pd, and Ba target nuclei at projectile energies between 18 and 29 MeV. Their analyses strongly support the interpretation of the two-nucleon-transfer reaction as an interference of one- and two-step mechanisms.

The investigation of Kato *et al.*<sup>7</sup> for the  $^{13}\text{C}(\vec{p}, t)$  and  $^{13}\text{C}(\vec{p}, ^3\text{He})$  reactions at 65 MeV is closer to ours in both target mass and projectile energy. Their ZR cross-section scaling factors are closer to unity but otherwise their results generally appear to be quite similar to ours. Analyzing-power predictions are of the same marginal

quality as those presented here. From both investigations it seems that the  $L=0$  transition for  $(\vec{p}, t)$  is especially problematic at higher energies. This is likely to be due to the large momentum and angular-momentum mismatch. The  $L=0$  analyzing-power data, in particular, are not reproduced by the DWBA.

In the present study, cross-section and analyzing-power angular distributions for the  $^{17}\text{O}(\vec{p}, t)^{15}\text{O}$  reaction were measured at 89.7 MeV. These new data were not well reproduced with either zero-range or finite-range one-step calculations. The underprediction of the cross sections by the FR one-step calculations by about a factor of 2 may be interpreted as an indication of strong higher-order contributions to the reaction mechanism.

For the two simple one-particle to one-hole transfers measured on  $^{17}\text{O}$ , the effects of the inclusion of  $(\vec{p}, d; d, t)$  two-step processes in second-order DWBA calculations were investigated in the zero-range approximation. The observed lack of significant improvement in the description of the data with the inclusion of these two-step terms is disappointing. A similar treatment for  $^{207}\text{Pb}(\vec{t}, p)^{209}\text{Pb}$  has also failed to lead to quantitative agreement.<sup>3</sup> Finite-range coupled-channels calculations could solve the normalization problem and should be performed as soon as such a code is available.

However, merely replacing zero-range calculations by finite-range, two-step calculations alone will not solve all the remaining problems. In a recent article, Austern and Kawai<sup>43</sup> argue that the conventional two-step DWBA model which considers only the bound  $^3S$  state of the intermediate deuteron is certainly incomplete since it ignores other very important contributions. By using a closure approach for the intermediate  $(pn)$  system, they are able to include the three-body continuum, the coupling among breakup states, and singlet deuteron states, without the need for coupled equations. They find a transition amplitude [Eq. (16)] of the form  $T=T(1)+T(2)$ , where  $T(1)$  is the conventional one-step term and  $T(2)$  is given by

$$T(2) = \langle \hat{\chi}_t^{(-)} \varphi_t | \Delta U | \varphi(1) \rangle (E^{(+)} - \epsilon - \bar{\epsilon} - K_R - U_{JS})^{-1} \\ \times \langle \varphi(1) | V_{p2} | \varphi_p \hat{\chi}_p^{(+)} \rangle .$$

This amplitude formally contains the intermediate (bound) deuteron contribution, but its magnitude is larger than the bound-deuteron limit. A major difference from the conventional two-step formalism is that the two-nucleon potential  $U_{JS}$  is much less absorptive than the commonly used deuteron elastic-scattering potential. The evaluation of the properly generalized and antisymmetrized amplitude  $T(2)$  is beyond the scope of this study. However, it is expected that the changes relative to the calculations discussed earlier in this paper will be large, particularly for the analyzing powers.

## ACKNOWLEDGMENTS

We wish to thank the cyclotron crew members of IUCF for their cooperation, W. R. Lozowski for the preparation of the targets, and Dr. D. J. Millener for his helpful contributions to this paper. This work was supported in part by the National Science Foundation.

- \*Present address: Department of Physics, Princeton University, Princeton, NJ 08544.
- <sup>1</sup>J. A. MacDonald, J. Cerny, J. C. Hardy, H. L. Harvey, A. D. Bacher, and G. R. Plattner, *Phys. Rev. C* **9**, 1694 (1974).
  - <sup>2</sup>M. Pignanelli, J. Gosset, F. Resmini, B. Mayer, and J. L. Escudie, *Phys. Rev. C* **8**, 2120 (1973).
  - <sup>3</sup>W. W. Daehnick, R. E. Brown, E. R. Flynn, R. A. Hardekopf, and J. C. Peng, *Bull. Am. Phys. Soc.* **26**, 579 (1981); in *Proceedings of The International Conference on Nuclear Structure, Amsterdam, 1982*, edited by A. van der Woude and B. J. Verhaar (European Physical Society, Amsterdam, 1982), Vol. 1, p. 278; W. W. Daehnick, R. D. Rosa, M. J. Spisak, R. E. Brown, E. R. Flynn, R. A. Hardekopf, and J. C. Peng, *Bull. Am. Phys. Soc.* **28**, 651 (1983).
  - <sup>4</sup>N. Hashimoto and M. Kawai, *Prog. Theor. Phys.* **59**, 1245 (1978).
  - <sup>5</sup>W. W. Daehnick, M. J. Spisak, J. R. Comfort, H. Hafner, and H. H. Duhm, *Phys. Rev. Lett.* **41**, 639 (1978); W. W. Daehnick, M. J. Spisak, and J. R. Comfort, *Phys. Rev. C* **23**, 1096 (1981).
  - <sup>6</sup>Y. Aoki, H. Iida, S. Kunori, K. Nagano, Y. Toba, and K. Yagi, *Phys. Rev. C* **25**, 1050 (1982); **25**, 1696 (1982); H. Iida, Y. Aoki, K. Hashimoto, K. Nagano, Y. Tagishi, Y. Toba, and K. Yagi, *ibid.* **29**, 328 (1984); K. Yagi, H. Iida, Y. Aoki, K. Hashimoto, and Y. Tagishi, *ibid.* **31**, 120 (1985).
  - <sup>7</sup>S. Kato, K. Okada, M. Kondo, K. Hosono, T. Saito, N. Matsuoka, T. Noro, S. Nagamachi, H. Shimizu, K. Ogino, Y. Kadota, and M. Nomura, *Phys. Rev. C* **25**, 97 (1982).
  - <sup>8</sup>W. P. Alford, R. N. Boyd, E. Sugarbaker, F. W. N. de Boer, R. E. Brown, and E. R. Flynn, *Phys. Rev. C* **27**, 1032 (1983).
  - <sup>9</sup>H. Segawa, K. Kubo, and A. Arima, *Phys. Rev. Lett.* **35**, 357 (1975).
  - <sup>10</sup>L. A. Charlton, *Phys. Rev. C* **14**, 506 (1976).
  - <sup>11</sup>M. Igarashi and K. Kubo, *Phys. Rev. C* **25**, 2144 (1982).
  - <sup>12</sup>W. T. Pinkston and G. R. Satchler, *Nucl. Phys.* **A383**, 61 (1982); M. A. Nagarajan and G. R. Satchler, *Phys. Rev. Lett.* **49**, 899 (1982); G. R. Satchler and W. T. Pinkston, *Nucl. Phys.* **A411**, 144 (1983); G. R. Satchler and W. T. Pinkston, *Phys. Lett.* **B134**, 7 (1984).
  - <sup>13</sup>J. R. Comfort and W. W. Daehnick, *Phys. Rev. Lett.* **50**, 1627 (1983).
  - <sup>14</sup>D. K. Olsen and R. E. Brown, *Nucl. Phys.* **A170**, 544 (1971).
  - <sup>15</sup>P. Schwandt, H. O. Meyer, W. W. Jacobs, A. D. Bacher, S. E. Vigdor, M. D. Kaitchuk, and T. R. Donoghue, *Phys. Rev. C* **26**, 55 (1982).
  - <sup>16</sup>E. J. Stephenson, private communication.
  - <sup>17</sup>N. K. Glendenning, *Annu. Rev. Nucl. Sci.* **13**, 191 (1963).
  - <sup>18</sup>I. S. Towner and J. C. Hardy, *Adv. Phys.* **18**, 401 (1969).
  - <sup>19</sup>J. R. Shepard, E. Rost, and P. D. Kunz, in *Polarization Phenomena in Nuclear Physics—1980 (Fifth International Symposium, Sante Fe)*, Proceedings of the Fifth International Symposium on Polarization Phenomena in Nuclear Physics, AIP Conf. Proc. No. 69, edited by G. G. Ohlson, R. E. Brown, N. Jarmie, M. W. McNaughton, and G. M. Hale (AIP, New York, 1981), p. 361.
  - <sup>20</sup>H. Nann, D. W. Miller, W. W. Jacobs, D. W. Devins, and W. P. Jones, Indiana University Cyclotron Facility Scientific and Technical Report, 1982, p. 117.
  - <sup>21</sup>J. R. Shepard, R. E. Anderson, J. J. Kraushaar, R. A. Ristinen, J. R. Comfort, N. S. P. King, A. Bacher, and W. W. Jacobs, *Nucl. Phys.* **A322**, 92 (1979).
  - <sup>22</sup>J. R. Comfort, *Comput. Phys. Commun.* **16**, 35 (1978).
  - <sup>23</sup>J. D. Brown, W. P. Jones, P. M. Lister, and H. Nann, private communication.
  - <sup>24</sup>W. W. Daehnick, J. D. Childs, and Z. Vrcelj, *Phys. Rev. C* **21**, 2253 (1980).
  - <sup>25</sup>R. Stock, R. Bock, P. David, H. H. Duhm, and T. Tamura, *Nucl. Phys.* **A104**, 136 (1967); R. M. DelVecchio and W. W. Daehnick, *Phys. Rev. C* **6**, 2095 (1972); J. R. Shepard, P. D. Kunz, and J. J. Kraushaar, *Phys. Lett.* **B56**, 135 (1975).
  - <sup>26</sup>F. D. Becchetti and G. W. Greenlees, in *Polarization Phenomena in Nuclear Reactions*, edited by H. H. Barschall and W. Haerberli (University of Wisconsin, Madison, 1971), p. 682.
  - <sup>27</sup>W. Bohne, H. Homeyer, H. Lettau, H. Morgenstern, and J. Scheer, *Nucl. Phys.* **A156**, 93 (1970).
  - <sup>28</sup>L. F. Hansen, M. L. Stelts, J. G. Vidal, J. J. Wesolowski, and V. A. Madsen, *Phys. Rev.* **174**, 1155 (1968).
  - <sup>29</sup>W. S. McEver, T. B. Clegg, J. M. Joyce, and E. J. Ludwig, in *Polarization Phenomena in Nuclear Reactions*, edited by H. H. Barschall and W. Haerberli (University of Wisconsin, Madison, 1971), p. 603.
  - <sup>30</sup>P. M. Lewis, A. K. Basak, J. D. Brown, P. V. Drumm, O. Karban, E. C. Pollacco, and S. Roman, *Nucl. Phys.* **A395**, 206 (1983).
  - <sup>31</sup>T. Tanabe, K. Koyama, M. Yasue, H. Yokomizo, K. Sato, J. Kokame, N. Koori, and S. Tanaka, *J. Phys. Soc. Jpn.* **41**, 361 (1976).
  - <sup>32</sup>Code FRUCK2, written by P. D. Kunz (unpublished); extended version by J. R. Comfort (unpublished).
  - <sup>33</sup>Code CHUCK3, written by P. D. Kunz (unpublished); extended version by J. R. Comfort (unpublished).
  - <sup>34</sup>Y. C. Tang, E. W. Schmid, and R. C. Herndon, *Nucl. Phys.* **65**, 203 (1965); Y. C. Tang and R. C. Herndon, *Phys. Lett.* **18**, 42 (1965).
  - <sup>35</sup>P. D. Kunz, private communication.
  - <sup>36</sup>B. F. Bayman and A. Kallio, *Phys. Rev.* **156**, 1121 (1967).
  - <sup>37</sup>S. Burzynski, M. Baumgartner, H. P. Gubler, J. Jourdan, H. O. Mayer, G. R. Plattner, H. W. Roser, I. Sick, and K. H. Moebius, *Nucl. Phys.* **A399**, 230 (1983).
  - <sup>38</sup>F. Ajzenberg-Selove, *Nucl. Phys.* **A360**, 1 (1981).
  - <sup>39</sup>G. R. Smith, J. R. Shepard, R. L. Boudrie, R. J. Peterson, G. S. Adams, T. S. Bauer, G. J. Igo, G. Pauletta, C. A. Whitten, Jr., A. Wriekat, B. Hoistad, and G. W. Hoffmann, *Phys. Rev. C* **30**, 593 (1984).
  - <sup>40</sup>D. J. Millener, private communication.
  - <sup>41</sup>W. W. Daehnick, *Phys. Rep.* **96**, 317 (1983).
  - <sup>42</sup>M. A. Nagarajan, M. R. Strayer, and M. F. Werby, *Phys. Lett.* **68B**, 421 (1977); D. H. Feng, M. A. Nagarajan, M. R. Strayer, M. Vallieres, and W. T. Pinkston, *Phys. Rev. Lett.* **44**, 1037 (1980).
  - <sup>43</sup>N. Austern and M. Kawai, *Phys. Rev. C* **31**, 1083 (1985).